Article

Cell Reports

YAP Inhibition Restores Hepatocyte Differentiation in Advanced HCC, Leading to Tumor Regression

Graphical Abstract

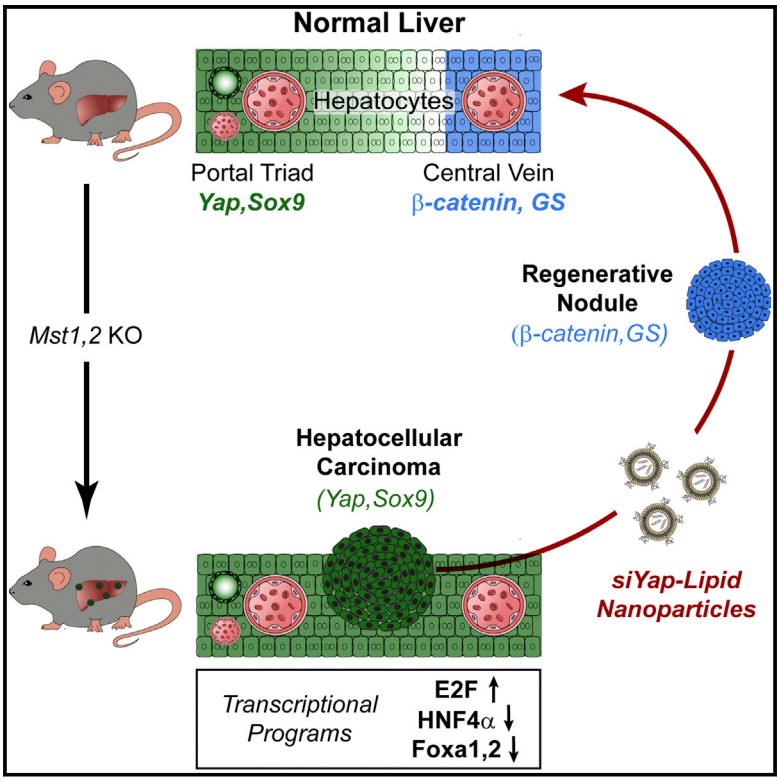

Highlights

- Yap is a rheostat for positional identity and metabolic zonation of hepatocytes
- Activated Yap subverts the HNF4α and β-catenin hepatocyte differentiation programs
- siYap-LNPs cause advanced HCC to regress and undergo hepatocyte differentiation
- An aggressive human HCC subtype with WT CTNNB1 exhibits a Yap activity signature

Authors

Julien Fitamant, Filippos Kottakis, ..., Lakshmi Raj, Nabeel Bardeesy

Correspondence

avruch@molbio.mgh.harvard.edu (J.A.), bardeesy.nabeel@mgh.harvard.edu (N.B.)

In Brief

Fitamant et al. show that the identity of specialized subpopulations of hepatocytes is controlled by Yap levels and that aberrant Yap activation overrides hepatocyte differentiation to initiate and maintain hepatocellular carcinoma (HCC) growth. In advanced HCC, Yap inhibition restores hepatocyte differentiation, supporting the concept of differentiation therapy against epithelial cancers.

Accession Numbers

GSE65665

Fitamant et al., 2015, Cell Reports *10*, 1692–1707
March 17, 2015 ©2015 The Authors
http://dx.doi.org/10.1016/j.celrep.2015.02.027

OPEN ACCESS
CellPress

Cell Reports
Article

YAP Inhibition Restores Hepatocyte Differentiation in Advanced HCC, Leading to Tumor Regression

Julien Fitamant,[1,2,4] Filippos Kottakis,[1,2,4] Samira Benhamouche,[1,5,6] Helen S. Tian,[1,2] Nicolas Chuvin,[1,2] Christine A. Parachoniak,[1,2,4] Julia M. Nagle,[1,2] Rushika M. Perera,[1,2,4] Marjorie Lapouge,[1,2] Vikram Deshpande,[1,5] Andrew X. Zhu,[1,4] Albert Lai,[7] Bosun Min,[7] Yujin Hoshida,[8] Joseph Avruch,[3,4,*] Daniela Sia,[8,9] Genís Campreciós,[8] Andrea I. McClatchey,[1,5] Josep M. Llovet,[8,10,11] David Morrissey,[7] Lakshmi Raj,[7] and Nabeel Bardeesy[1,2,4,*]

[1]Cancer Center
[2]Center for Regenerative Medicine
[3]Department of Molecular Biology
Massachusetts General Hospital, 185 Cambridge Street, Boston, MA 02114, USA
[4]Department of Medicine
[5]Department of Pathology
Harvard Medical School, Boston, MA 02114, USA
[6]Inserm U1053, University of Bordeaux, 146 rue Leo Saignat, 33076 Bordeaux Cedex, France
[7]Novartis Institutes of Biomedical Research Inc., 250 Massachusetts Avenue, Cambridge, MA 02139, USA
[8]Liver Cancer Program, Tisch Cancer Institute, Division of Liver Diseases, Department of Medicine, Icahn School of Medicine at Mount Sinai, New York, NY 10029, USA
[9]Gastrointestinal Surgery and Liver Transplantation Unit, National Cancer Institute, Milan 20133, Italy
[10]HCC Translational Research Laboratory, BCLC Group, Liver Unit, IDIBAPS, Hospital Clínic, CIBERehd, Universitat de Barcelona, 08036 Barcelona, Catalonia, Spain
[11]Institució Catalana de Recerca i Estudis Avançats (ICREA), 08010 Barcelona, Catalonia, Spain
*Correspondence: avruch@molbio.mgh.harvard.edu (J.A.), bardeesy.nabeel@mgh.harvard.edu (N.B.)
http://dx.doi.org/10.1016/j.celrep.2015.02.027

SUMMARY

Defective Hippo/YAP signaling in the liver results in tissue overgrowth and development of hepatocellular carcinoma (HCC). Here, we uncover mechanisms of YAP-mediated hepatocyte reprogramming and HCC pathogenesis. YAP functions as a rheostat in maintaining metabolic specialization, differentiation, and quiescence within the hepatocyte compartment. Increased or decreased YAP activity reprograms subsets of hepatocytes to different fates associated with deregulation of the HNF4A, CTNNB1, and E2F transcriptional programs that control hepatocyte quiescence and differentiation. Importantly, treatment with small interfering RNA-lipid nanoparticles (siRNA-LNPs) targeting YAP restores hepatocyte differentiation and causes pronounced tumor regression in a genetically engineered mouse HCC model. Furthermore, YAP targets are enriched in an aggressive human HCC subtype characterized by a proliferative signature and absence of *CTNNB1* mutations. Thus, our work reveals Hippo signaling as a key regulator of the positional identity of hepatocytes, supports targeting of YAP using siRNA-LNPs as a paradigm of differentiation-based therapy, and identifies an HCC subtype that is potentially responsive to this approach.

INTRODUCTION

Hepatocellular carcinoma (HCC) is the second most common cause of cancer-related deaths worldwide, and the incidence is increasing in the United States (El-Serag, 2011; Forner et al., 2012). Curative resection or transplantation is only possible in ~30% of patients, and for advanced HCC, the multi-kinase inhibitor sorafenib remains the only approved agent with modest survival benefits (Cheng et al., 2009; Llovet et al., 2008). Genomic studies have classified HCC into subsets with distinct molecular and clinical features (Chiang et al., 2008; Guichard et al., 2012; Hoshida et al., 2009; Lachenmayer et al., 2012). Activating *CTNNB1* mutations are the most common oncogenic drivers (being present in ~30% of tumors) and define an HCC subtype characterized by a hepatocyte-like gene-expression signature, well-differentiated histology, and improved survival. The other recurrent genetic alterations in HCC involve tumor-suppressor inactivation (Fujimoto et al., 2012; Guichard et al., 2012) and have not pointed to readily targetable vulnerabilities. Thus, there is a need to more fully discern biologically distinct HCC subtypes and to identify therapeutic targets.

Hippo signaling is an important tumor-suppressor mechanism in multiple tissues, including the liver (Harvey et al., 2013; Mo et al., 2014). The core of the pathway involves a kinase cascade with the homologous MST1 and MST2 (STK3 and STK4) proteins as upstream kinases that subsequently activate the LATS1/LATS2 kinases (Yu and Guan, 2013). Signaling inputs include G protein-coupled receptors, Rho GTPases, AMPK, and polarity complex proteins such as NF2, AMOT, and α-CATENIN, which

link Hippo activity to a variety of cues, including cell contact, mitotic failure, nutrients, and growth factors (Ganem et al., 2014; Yu and Guan, 2013). Major downstream targets are the transcriptional co-activators YAP and TAZ, which are phosphorylated by LATS1/LATS2, leading to their cytoplasmic retention and degradation. YAP and TAZ promote growth, survival, and/or stem cell-like phenotypes in many cellular contexts (Mo et al., 2014), although the key mediators of these processes are not clearly established.

In the adult mouse liver, inactivation of *Mst1/Mst2*, *Sav1*, or *Nf2*, or ectopic expression of *Yap* results in expansion of atypical ductal cells (ADCs, or "oval cells"), liver enlargement, and progression to HCC or mixed HCC/cholangiocarcinoma, and *Mst1/Mst2* KO or *Yap* overexpression also causes hepatocyte overproliferation (Camargo et al., 2007; Dong et al., 2007; Lee et al., 2010; Lu et al., 2010; Yimlamai et al., 2014; Zender et al., 2006; Zhou et al., 2009). Lineage tracing in *Yap* transgenic and *Nf2* KO livers indicates that ADCs are derived from de-differentiation of hepatocytes (Yimlamai et al., 2014), consistent with emerging data demonstrating plasticity of these cells (Schaub et al., 2014; Yanger et al., 2014), and pointing to important functions of Hippo/YAP in controlling liver cell fate. Consistent with a role for activated YAP in human HCC, ~50% of these tumors exhibit nuclear YAP staining, and nuclear YAP levels correlate with decreased survival after resection (Tschaharganeh et al., 2013; Xu et al., 2009).

Here, we sought to explore the role of YAP in HCC progression and maintenance in order to define its downstream oncogenic program, assess its potential as a therapeutic target, and establish biomarkers to identify the subsets of HCC in which YAP targeting may be beneficial. By using genetic approaches and small interfering RNA-lipid nanoparticle (siRNA-LNP) technology in genetically engineered mouse (GEM) models, we demonstrate that activation of endogenous YAP perturbs hepatocyte differentiation and maintains this state in advanced tumors. Correspondingly, YAP silencing in HCC restores hepatocyte differentiation and leads to tumor regression. These results provide a proof-of-concept that differentiation therapy has potential as a treatment strategy for epithelial tumors. Moreover, the significant responses induced by siYAP-LNPs support ongoing clinical development of this therapeutic modality. Finally, our work shows that an aggressive subtype of human HCC, enriched for cell-cycle gene expression and lacking *CTNNB1* mutations, exhibits a YAP activation signature, pointing to biomarkers to guide the deployment of YAP-directed therapies in clinical trials.

RESULTS

Role of YAP Downstream of MST1/MST2 in Controlling Hepatocyte Identity

To begin to explore the relationship between Hippo pathway activity and liver cell differentiation, we examined Yap expression in normal mouse liver. The bile ducts showed strong nuclear YAP staining (Figures 1A and 1B), consistent with prior observations (Yimlamai et al., 2014). We also observed a graded staining pattern in the hepatocyte compartment, with the periportal hepatocytes (adjacent to the bile duct) showing readily detectable Yap nuclear and cytoplasmic localization, and with pericentral hepatocytes (adjacent to the central vein) showing clear nuclear exclusion. SOX9, which like YAP is a marker of bile ducts and liver cell plasticity (Antoniou et al., 2009; Shin et al., 2011; Yanger et al., 2013), exhibited a similar expression pattern in hepatocytes along the porto-central axis (Figures 1A and S1A). This staining gradient is suggestive of a role for YAP in the zonation of hepatocytes, which have specialized metabolic functions depending on their position in the liver lobule (Jungermann and Katz, 1989). The zonation program is thought to be governed by the interplay of the HNF4A and WNT/β-CATENIN pathways and is characterized by strict boundaries of expression of key metabolic genes in the pericentral region and periportal regions (e.g., glutamine synthase and glutaminase 2, respectively) (Benhamouche et al., 2006; Gougelet et al., 2014; Torre et al., 2011).

To study the impact of Hippo pathway modulation on liver cell identity and proliferation, we generated mice with liver-specific *Mst1/Mst2* double-knockout (DKO), *Yap* deletion (Yap KO), and DKO combined with hemizygous or homozygous *Yap* deletion (designated DKO Yap+/− and triple-knockout [TKO] mice, respectively) via crosses of floxed strains to *Albumin-Cre* mice. Necropsy at 7 weeks revealed that DKO mice had massive liver overgrowth and high levels of hepatocyte proliferation, associated with upregulation of nuclear and total Yap levels throughout the hepatocyte compartment and marked expansion of SOX9+ and SOX9− ADCs in the periportal region (Figures 1C, S1B, and S1C), as previously reported in other Hippo pathway mutant mouse models (Benhamouche et al., 2010; Lee et al., 2010; Lu et al., 2010; Yimlamai et al., 2014). In addition, DKO animals exhibited a striking loss of hepatocyte zonation as reflected by decreased pericentral expression of glutamine synthase (GS) and ornithine aminotransferase (OAT) (Figures 1C, 1D, and S1D). Each abnormality was rescued in DKO Yap+/− and TKO mice, although the latter exhibited biliary defects, regional hepatocyte necrosis, cholestasis, fibrosis, and swelling of the tissue as observed in Yap KO livers (Zhang et al., 2010). Notably, in Yap KO mice, we found expansion of the GS+ domain, such that several layers of hepatocytes surrounding the central vein, as well as scattered cells throughout the lobule, showed aberrant induction of GS (Figure 1D). These findings link aberrantly activated YAP to hepatocyte reprogramming downstream of MST1/MST2 and reveal an unexpected role of basal YAP function in maintenance of hepatocyte zonation.

Despite the ongoing expansion of ADCs, proliferating cells with hepatocyte morphology persisted in the DKO liver and exhibited a higher frequency of proliferating cell nuclear antigen (PCNA) staining than adjacent ADCs (Figure S1C). Together, these data imply that the response of hepatocytes to activation of endogenous YAP is distinct depending on their zonal location, creating a highly proliferative population of dedifferentiated (GS−) pericentral hepatocytes as well as an expanded pool of ADCs emerging from periportal hepatocytes.

Acute Deregulation of the Hippo Pathway Overrides Hepatocyte Zonation

We recapitulated the above phenotypes in the setting of acute deregulation of the Hippo pathway using intravenous injection of Cre adenovirus to conditionally delete *Mst1/Mst2* and *Yap* in

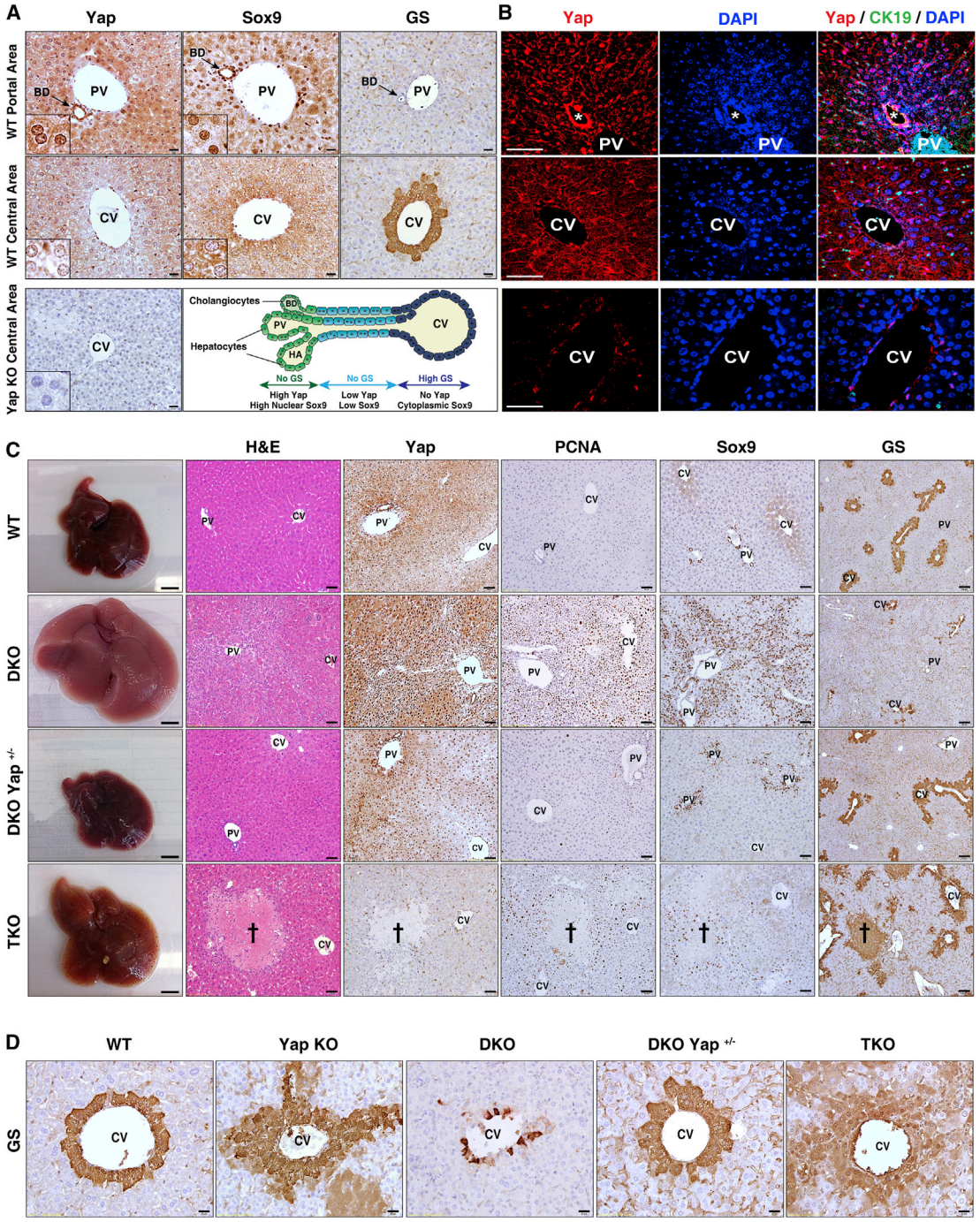

Figure 1. Hippo Signaling Is a Rheostat that Controls Hepatocyte Identity

(A and B) IHC (A) and immunofluorescence (B) of mouse liver in the region of the portal vein (top row) and central vein (middle row), demonstrating nuclear and cytoplasmic YAP staining in bile ducts (arrow) and periportal hepatocytes, and absence of YAP in the first layer of pericentral hepatocytes. SOX9 shows nuclear staining in bile ducts and weaker nuclear staining in periportal hepatocytes, whereas it is excluded from the nucleus in pericentral hepatocytes. GS is a pericentral marker. CK19 is a biliary marker. The schematic representation of the porto-central axis indicates the territories of expression for YAP, SOX9, and GS. Yap KO liver (bottom row) is a negative control for YAP staining. Insets show magnified periportal or pericentral hepatocytes in (A). Bile duct is indicated by an asterisk in (B). Scale bars, 20 μm (A) and 50 μm (B).

(C) Gross, histologic, and IHC analyses of livers of the indicated genotypes (Albumin-Cre models). Cross: necrotic region in TKO. Scale bars, 5 mm (gross), 50 μm (H&E, YAP, PCNA, and SOX9), and 100 μm (GS).

(D) GS staining in pericentral regions. Scale bar, 20 μm.

PV, portal vein; CV, central vein; BD, bile duct; HA, hepatic artery. See also Figure S1.

adult hepatocytes (designated as the DKO^{Ad}, TKO^{Ad}, and Yap KO^{Ad} models). An examination at 2 weeks post-injection revealed that DKO^{Ad} mice had increased hepatocyte proliferation, ADC expansion, and reduced pericentral GS expression compared with wild-type (WT)^{Ad} livers (Figures 2A–2C). These changes were rescued by *Yap* ablation (TKO^{Ad} and DKO Yap+/−^{Ad} models); moreover, Yap KO^{Ad} mice exhibited expansion of the GS+ domain (10.1% ± 0.5% of hepatocytes were GS+ in WT^{Ad} livers versus 16.0% ± 0.9% in Yap KO^{Ad}, and 8.0% ± 0.5% in DKO^{Ad}; Figure 2C; see Supplemental Experimental Procedures). Thus, YAP serves as a rheostat for maintaining quiescence and identity in adult hepatocytes. In particular, activation of YAP overrides the pericentral zonation program and also directs periportal hepatocytes to dedifferentiate to ADCs, whereas basal levels of Yap are required to prevent the aberrant induction of a pericentral phenotype in multiple layers of hepatocytes surrounding the central vein.

We conducted gene-expression profiling at day 8 following Ad-Cre administration to determine the early transcriptional changes provoked by *Mst1/Mst2* inactivation (WT^{Ad} versus DKO^{Ad}). Gene set enrichment analysis (GSEA) revealed that acute *Mst1/Mst2* DKO caused potent inactivation of the hepatocyte differentiation program, with downregulation of hundreds of hepatocyte-specific genes (Figure 2D). Accordingly, the set of downregulated genes was highly enriched for established targets of the master regulators of hepatocyte identity, HNF4A and FOXA2. Conversely, there was upregulation of cell-proliferation signatures enriched for E2F target genes (Figure 2E). Experimentally determined binding sites for TEAD/TEF-1 were significantly enriched in the promoter elements of the differentially expressed genes ($p < 2.0 \times 10^{-14}$), as was the consensus TEAD/TEF1 binding motif (Figure S2A), consistent with TEAD family proteins being the key partners for YAP in the liver (Liu-Chittenden et al., 2012). We identified candidate direct YAP targets by integrating the expression analysis and chromatin immunoprecipitation (ChIP) data for TEAD binding in hepatic cells (HepG2 cells, ENCODE database; Figure S2B; Table S1). This gene set was highly enriched for predicted targets of HNF4A and FOXA1, which are master regulators of hepatocyte differentiation that cooperatively regulate many common targets (Figure S2B; Alder et al., 2014; Bochkis et al., 2012; Li et al., 2012). Notably, YAP has been shown to act as a switch for enhancer occupancy of HNF4A and FOXA2 in the liver, preventing expression of mature hepatocyte genes and promoting expression of liver stem cell (hepatoblast) genes (Alder et al., 2014). Moreover, deletion of *Hnf4a* in the adult liver results in hepatocyte dedifferentiation and the emergence of SOX9+ ADCs (Saha et al., 2014; Walesky et al., 2013). These observations suggest a potential mechanism involving an interplay between activated YAP and an HNF4A/FOXA2/FOXA1 module for the control of hepatocyte identity and quiescence in DKO mice.

Yap Status Dictates HCC Cell Differentiation Phenotypes Downstream of Hippo Inactivation

We next sought to assess the effects of YAP deficiency on the tumor phenotype caused by *Mst1/Mst2* DKO (Lu et al., 2010; Zhou et al., 2009). To this end, mice were either necropsied at serial time points or monitored until signs of poor body condition necessitated euthanasia, which in all cases was due to the presence of liver tumors. At 15 weeks, DKO mice had rampant ADC expansion, whereas DKO Yap+/− and TKO livers showed only a focal appearance of hepatocyte-like cells staining strongly for SOX9, and limited or no cells with ADC morphology (Figure 3A). In addition, TKO and DKO Yap+/− mice had a marked extension in survival as compared with DKO animals (48.1 and 59.4 weeks versus 23.5 weeks, respectively), as well as a reduced tumor burden (TKO 11 tumors/mouse; DKO Yap+/− 10 tumors/mouse, DKO 39 tumors/mouse; Figures 3B and 3C). Immunohistochemistry (IHC) confirmed that TKO tumors lacked Yap expression, indicating that they did not emerge from rare cells that escaped *Yap* deletion (Figure 3E, lower panel). Thus, Yap has a central role in tumorigenesis in the DKO model and even single-copy *Yap* ablation greatly delays HCC progression. On the other hand, results from TKO mice demonstrate that *Mst1/Mst2* inactivation can still ultimately drive liver tumorigenesis through a YAP-independent, albeit less potent, program.

Histopathologic analysis at end stage revealed that the tumors in each genotype were invasive HCC (Figure 3E). However, the groups expressed distinct sets of differentiation markers, with the DKO HCCs staining for SOX9 and lacking both GS and nuclear β-CATENIN, and the great majority of TKO and DKO Yap+/− tumors showing the opposite profile (Figures 3D and 3E). The phenotypes caused by liver-specific inactivation of *Nf2*, which are partially due to YAP activation, overlap those observed in DKO mice (Benhamouche et al., 2010; Yin et al., 2013; Zhang et al., 2010). An examination of *Nf2* KO HCCs revealed heterogeneous YAP staining in sharply demarcated regions. Those with higher nuclear and cytoplasmic YAP expressed SOX9 and lacked GS, whereas those with lower levels of YAP staining showed a reciprocal pattern (Figure S3A), again correlating YAP levels and markers of the HCC differentiation state. Together, these findings suggest a link between YAP-dependent hepatocyte reprogramming and HCC initiation, and connect YAP activity to the specific malignant phenotype of the ensuing tumors.

Therapeutic Efficacy of siRNA-LNPs Targeting YAP in Advanced HCC

We next explored the functions of YAP in the clinically relevant setting of maintenance of established tumors. In this regard, the use of siRNA encapsulated into LNPs (siLNPs), which improves the cellular uptake, stability, and pharmacokinetics of the siRNA (Whitehead et al., 2009), is an approach to YAP targeting with clinical potential. Primary HCC is a particularly plausible cancer context for the use of siRNA-LNP because the dual blood supply and fenestrated endothelium in the liver lead to high perfusion, which may facilitate siRNA-LNP delivery. To test this strategy, we developed protocols to monitor tumor development in the DKO^{Ad} model by ultrasound (US) imaging. Pilot studies with serial imaging followed by necropsy provided histologic verification that the lesions detected by US were invasive HCC (Figure 4A). Subsequently, an additional cohort was imaged, and animals with comparable tumor burden were randomized to receive tail-vein injections of siLNPs targeting YAP or a luciferase (Luc) control (Figure 4B). Mice were

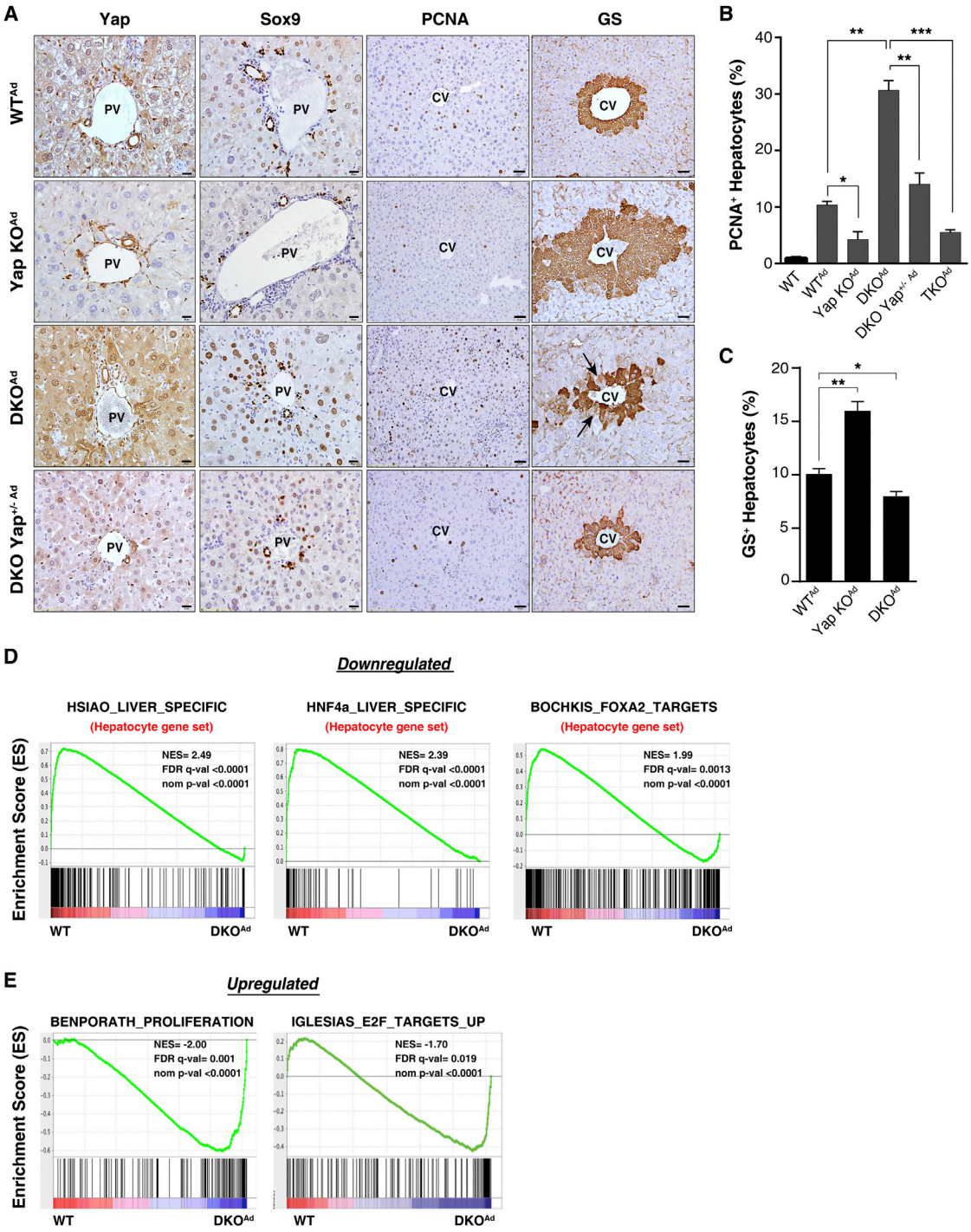

Figure 2. Acute Effect of Hippo Pathway Modulation on Hepatocyte Identity

(A–C) Mice were administered Cre adenovirus intravenously and livers were analyzed 2 weeks later by IHC for YAP, SOX9, PCNA, and GS. The graphs quantify PCNA (B) and GS (C) staining. n = 3 mice in the WT, WT^{Ad}, Yap KO^{Ad}, and TKO^{Ad} groups; 4 mice in the DKO Yap$^{+/-\ Ad}$ group; and 5 mice in the DKO^{Ad} group. Error bars indicate SEM. *p < 0.05, **p < 0.01, ***p < 0.001, ****p < 0.0001. Scale bars, 20 μm (YAP and SOX9) and 50 μm (PCNA and GS).

(D and E) GSEA of mRNA expression data after acute deletion of *Mst1*/*Mst2* in liver. DKO and WT mice were administered Adeno-Cre, and liver mRNA was isolated after 8 days.

(D) GSEA revealed rapid loss of a broad program of hepatocyte differentiation genes and targets of the master hepatocyte regulators HNF4A and FOXA2.

(legend continued on next page)

euthanized after 4 and 9 days to assess the acute responses. Quantitative RT-PCR (qRT-PCR) and IHC revealed progressive YAP knockdown by siYap-LNPs (Figures 4C–4E and S4A). At day 4, IHC showed that 45% of tumor nodules had a partial or complete reduction in YAP protein (Figures 4E and S4A; defined as % of HCC cells within the nodule staining above background; see Figure S4B and Supplemental Experimental Procedures), and by day 9 this figure increased to 73.5% of nodules (29.4% partial, 44.1% complete; Figures 4D and 4E). We also observed a coordinate reduction in expression of Ctgf, an established YAP-TEAD target, as well as of a series of E2F targets (Figure 4C).

Importantly, siYAP-LNP treatment resulted in a prominent decrease in tumor cell proliferation that was proportional to the degree of knockdown at both day 4 and 9, as determined by KI67 and PCNA staining (Figures 4D, 4F, S4A, and S4B). At day 9, 25.5% ± 1.6% of HCC cells in siLuc-LNP treated controls stained for proliferation markers, whereas the rates in the siYAP-LNP-treated group were 2.9% ± 0.4% and 11.8% ± 1.1% in nodules with complete or partial Yap knockdown, respectively (Figures 4D and 4F). There was no evidence of apoptosis as determined by cleaved caspase-3 staining (Figure S4A). These findings were corroborated using a second siLNP targeting a different YAP sequence (siYAP-LNP#2; Figure S4C) and reveal a critical function of YAP in the proliferation of advanced HCC in this model.

To identify the transcriptional program underlying YAP-mediated tumor maintenance, we conducted RNA-sequencing (RNA-seq) on siLuc- and siYAP-treated tumors following 9 days of treatment. GSEA revealed that YAP silencing caused potent inactivation of the E2F/cell proliferation pathway (Figures 4G and S4D, left panel). Reciprocally, there was a pronounced induction of a hepatocyte differentiation signature (Figure 4H, left panel), including activation of a program of specific pericentral hepatocyte markers (Figure 4H, right panel), and enrichment of predicted HNF4A targets (Figure S4D, right panel). We integrated the set of genes that were altered by siYAP-LNP treatment in HCCs with ChIP data for TEAD occupancy in liver cancer cells in order to identify candidate direct YAP/TEAD target genes in these tumors (see Experimental Procedures). To gain further insight into transcriptional circuits, we then searched this YAP/TEAD signature for enrichment of known binding sites for other transcription factors using the ENCODE database (Figure S4E; Table S2). In line with our observations in the DKO liver, the YAP/TEAD signature was greatly enriched for HNF4 and FOXA1 binding sites, which were ranked first and second among all transcription factors analyzed, consistent with the interplay between these factors in dictating the balance between tumor maintenance and hepatocyte differentiation (Figure S4E).

A comparison of the day 4 and day 9 time points indicated that the differentiation markers were gradually induced. At day 4, multiple HCC nodules with patchy staining for GS and nuclear β-CATENIN were observed in siYAP-LNP-treated mice, with positively stained regions correlating with areas of more complete YAP knockdown (Figure S4F). By day 9, uniform staining for both markers was frequently observed, coordinated with loss of SOX9 (Figure 4I). Thus, YAP inhibition in aggressive HCC causes rapid downregulation of the E2F cell-cycle pathway and progressive induction of a hepatocyte differentiation program associated with upregulation of HNF4/FOXA2/FOXA1 targets and increased activity of the pericentral/β-CATENIN program.

siYAP-LNPs Induce a Hepatocyte Differentiation Program in Advanced HCC

Tumor-bearing mice were treated with siRNA-LNPs for 4 weeks and then euthanized to determine the durability of the response and uncover any gradual consequences for tumor phenotypes. Consistent with the profound anti-proliferative effects seen upon acute YAP knockdown, the siYAP-LNP-treated animals showed a dramatic reduction in tumor burden as compared with controls, with marked decreases in the number of HCCs (9.9 versus 0.5) and their total cross-sectional area (9.2×10^6 μm^2 versus 0.75×10^6 μm^2; Figure 5A). Adjacent regions of liver tissue showed restoration of zonal GS expression and complete elimination of ADCs (Figure 5B). Remarkably, siYAP-LNP treatment resulted in the replacement of virtually all invasive HCCs by areas of cells resembling regenerative hepatocyte nodules. In comparison with the HCCs in control animals, these cells had a lower nuclear-to-cytoplasmic ratio, lacked mitotic figures, and showed a reduction in cell-plate thickness (Figure 5C). Correspondingly, these nodules had low proliferation rates and showed induction of GS and nuclear β-catenin (Figures 5C and 5D). Thus, sustained YAP inhibition provoked a broad hepatocyte differentiation program in established tumors.

The rare remaining HCC foci in siYAP-LNP-treated animals exhibited persistent YAP expression, suggesting that resistance arose either from augmented YAP expression or altered uptake or activity of the siRNA-LNPs (Figure S5A). Importantly, the treatment regimen was well tolerated. It caused no weight loss or significant changes in liver function values, and there was a slight inflammation in periportal areas that was fully resolved within 2–4 weeks following discontinuation of treatment (Figures S5B–S5D). These data indicate a central function of YAP in HCC tumor maintenance in the DKO model and support the application of siLNPs targeting YAP to treat advanced HCC. In addition, these studies provide a proof-of-concept for differentiation therapy as an oncologic approach in the context of an aggressive epithelial tumor.

YAP-Mediated Control of Proliferative and Hepatic Differentiation Programs in Primary Tumor Cultures

We used a series of early-passage HCC tumor cultures derived from independent DKO and TKO mice to examine in vitro the relationship between Yap activity and proliferation and

(E) GSEA showed strong induction of a proliferation gene signature including established E2F targets. Liver-derived gene sets are indicated in red. NES, normalized enrichment score; FDR, false-discovery rate. Gene sets were obtained from the Molecular Signatures Database, except for (HNF4a_LIVER_SPECIFIC), which is a curated list of liver-specific HNF4A targets (Saha et al., 2014).
See also Figure S2 and Table S1.

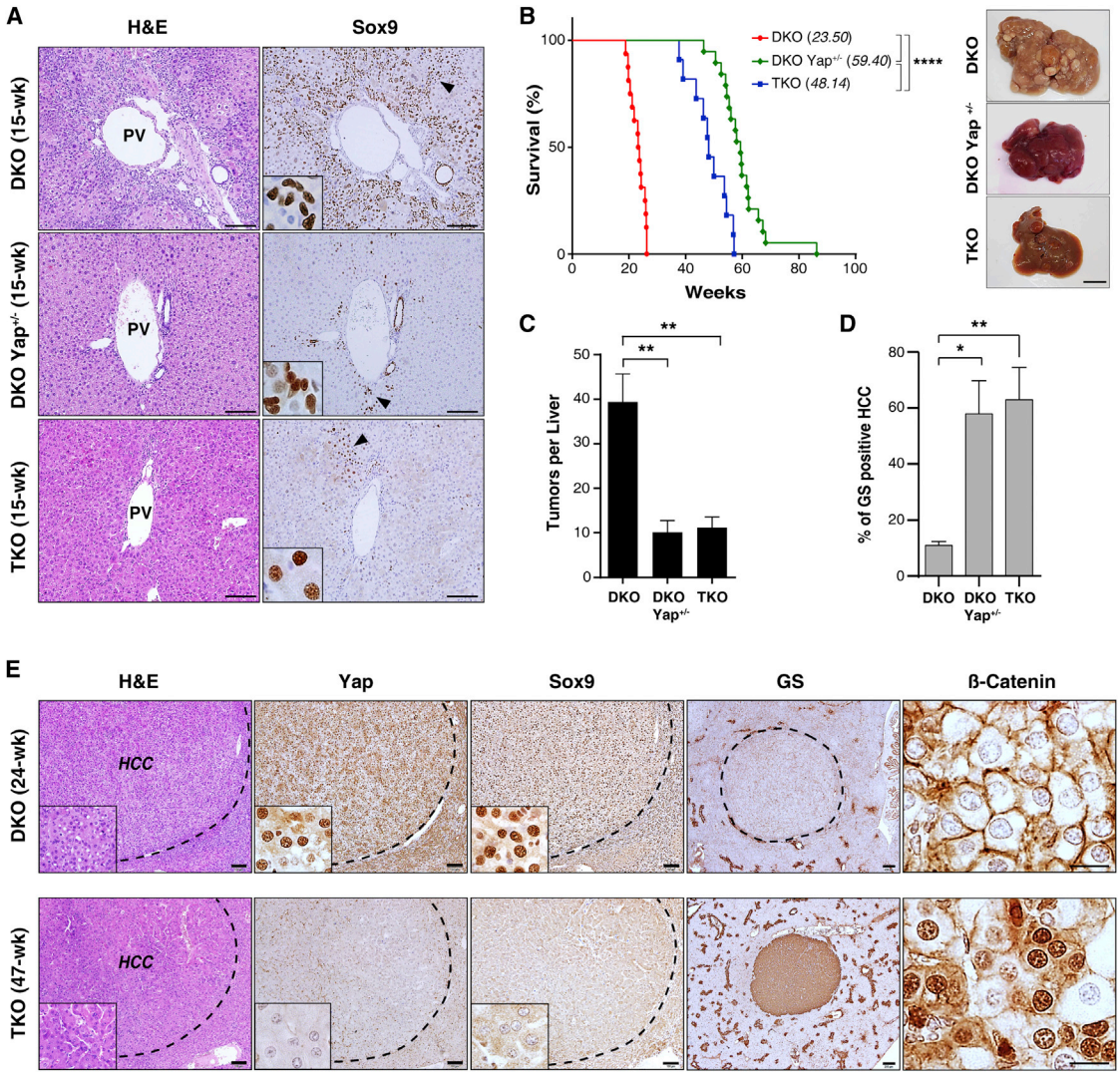

Figure 3. YAP Suppresses the β-CATENIN Pericentral Program and Drives Invasive HCC Downstream of Mst1/Mst2 DKO

(A) Analysis of the indicated genotypes by H&E and SOX9 staining at 15 weeks. The dedifferentiation of hepatocytes to ADCs caused by *Mst1/Mst2* DKO is blocked by hemizygous or homozygous Yap deletion, although scattered SOX9+ cells are observed by this time point. Insets: high-magnification images of regions denoted by arrowheads in the main panels. Note differences in the morphology of SOX9+ cells between genotypes. Scale bar, 100 μm.

(B) Left panel: Kaplan-Meier analysis showing the time until animals reached endpoints for disease burden and required euthanasia (see Experimental Procedures). Median survival is indicated in brackets. n = 16 mice (DKO), 19 mice (DKO Yap$^{+/-}$), and 11 mice (TKO). ****$p < 0.0001$. Right panels: gross images of representative livers at sacrifice.

(C) Mean tumor burden at sacrifice. n = 8 mice (DKO), 7 mice (DKO Yap$^{+/-}$), and 7 mice (TKO). Error bars indicate SEM. **$p < 0.01$.

(D and E) Histologic and IHC analyses of tumors from DKO and TKO mice with end-stage disease.

(D) Quantification of GS staining; n = 4 mice per group. Error bars indicate SEM.*$p < 0.05$ and **$p < 0.01$. All tumors showed HCC histopathology, although distinct staining patterns were noted for liver markers.

(E) Top: DKO tumors stained positive for SOX9 and negative for GS and nuclear β-catenin (top), whereas the majority of TKO tumors (bottom) showed the opposite pattern. All TKO tumors lacked YAP staining. Scale bars, 20 μm (β-catenin), 100 μm (H&E, YAP, and SOX9), and 200 μm (GS).

See also Figure S3.

differentiation pathways. Consistent with our in vivo data, DKO tumor cultures grew more rapidly than TKO cultures and were characterized by higher expression of multiple E2F-regulated cell-cycle genes and lower expression of a set of HNF4A targets involved in specialized hepatocyte functions (Figures 6A and 6B). Likewise, YAP knockdown in DKO cells caused proliferative arrest without evidence of cell death, whereas TKO cells were unaffected, demonstrating the specificity of the RNAi (Figures 6C and S6A). The YAP-depleted DKO cells exhibited reduced expression of E2F target genes and pronounced activation of the HNF4A gene signature (Figure 6D). Reciprocally, forced expression of YAP promoted the proliferation of TKO cultures

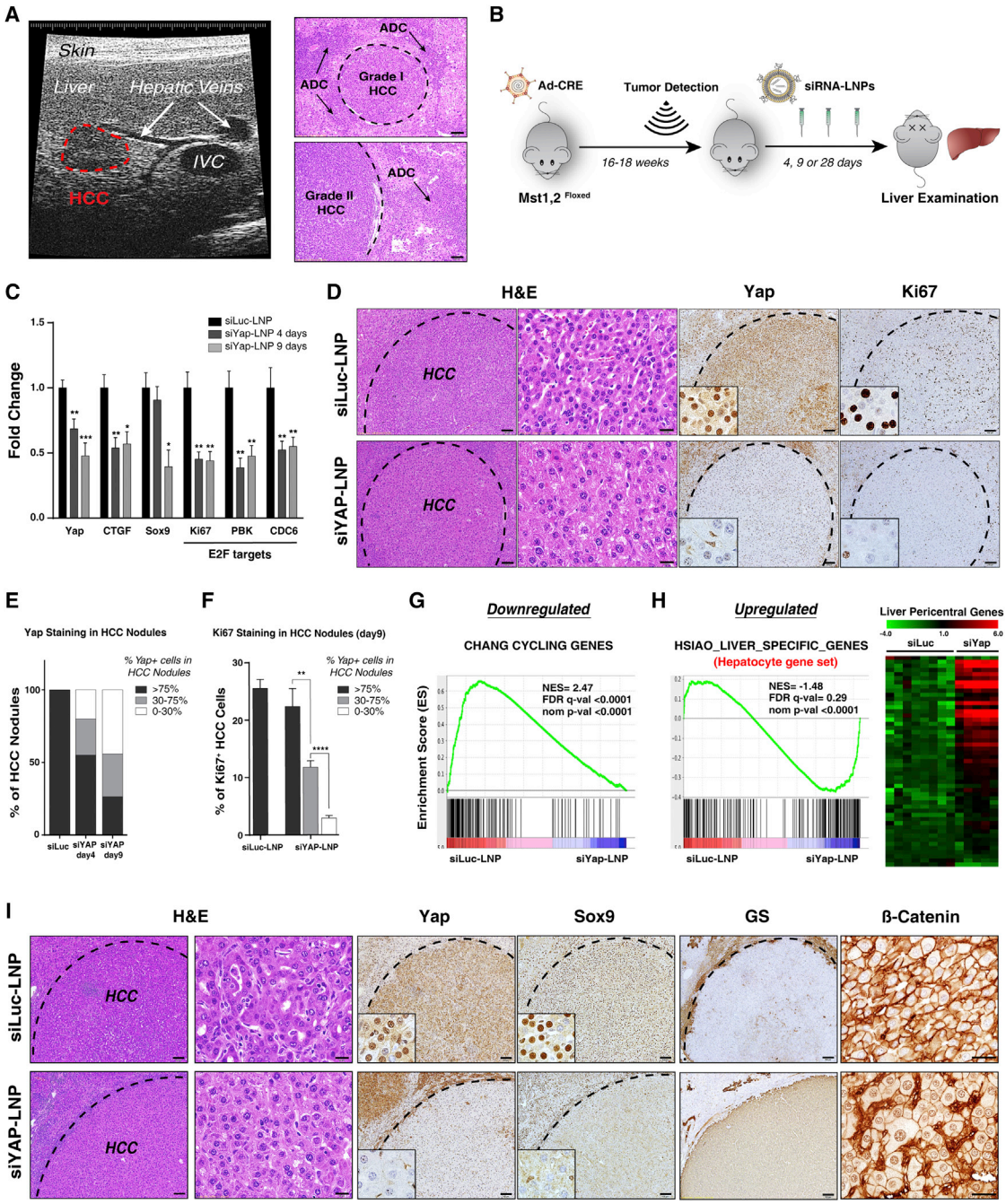

Figure 4. siLNP-Mediated YAP Silencing Induces Proliferative Arrest and a Pericentral Hepatocyte Differentiation Program in Advanced HCC

(A) Ultrasound (US) detection of a liver tumor in DKO^{Ad} at 16 weeks after Adeno-Cre injection. The right panel shows corresponding histology of liver tumors. IVC, interior vena cava. Scale bar, 100 μm.

(B) Schematic of the therapeutic study. Upon detection of tumors by US imaging, animals were randomized into groups receiving siYAP-LNPs or control siLuc-LNPs, and euthanized at the indicated time points.

(C) qRT-PCR analysis of tumors isolated after 4 or 9 days of treatment. n = 32 tumors (siLuc), 18 tumors (siYAP 4 days), and 16 tumors (siYAP 9 days). Error bars indicate SEM. *p < 0.05, **p < 0.01, ***p < 0.001.

(D) Representative IHC staining for YAP and KI67 in HCCs following 9 days of treatment. Note that at 9 days, HCC cells are preferentially targeted by siYAP-LNPs, whereas all liver cells show knockdown at later time points (see Figure 5C). Scale bars, 20 μm (H&E [right]) and 100 μm (H&E [left], YAP, and KI67).

(E) Quantification of YAP staining in HCC nodules at days 4 and 9. The chart shows the percentage of HCC nodules containing the indicated proportions of YAP+ tumor cells (black, >75% of cells YAP+; gray, 30%–75%; white, 0%–30%). Note that YAP knockdown efficiency increases from day 4 to day 9.

(legend continued on next page)

(referred to as TKO-Yap cells), whereas it either slowed or did not affect the proliferation DKO cells that already harbored high YAP levels (Figure 6E and data not shown). The TKO-Yap cells showed a corresponding induction of the E2F target and suppression of the HNF4A targets (Figure 6F). Finally, we found that TKO-Yap cells were sensitized to the CDK4 inhibitor PD-0332991 at concentrations that did not affect TKO-control cells (Figures 6G and S6B). Thus, the role of YAP in sustaining proliferation and blocking differentiation is recapitulated in cultured HCC cells and points to direct functional roles for YAP in activating E2F and suppressing HN4A activity in these tumors.

YAP Activation Is Associated with the Proliferative, CTNNB1 Wild-Type Subclass of HCC in Humans

Mutations in *CTNNB1* define a distinct subtype of HCC with less aggressive clinical features (Chiang et al., 2008). Since we observed an inverse correlation between YAP and β-CATENIN activity in the DKO HCC model, our data predict that YAP activation and *CTNNB1* mutations may be associated with different HCC subtypes. In this regard, it is notable that nuclear β-catenin staining, which is closely correlated with *CTNNB1* mutations, and nuclear YAP staining showed a strong negative association in human HCC specimens (Tao et al., 2014). We sought to extend these data by using our YAP activity signature to identify HCC subtypes potentially driven by YAP. We derived this signature of presumptive direct YAP targets by integrating the set of genes that were altered by siYAP-LNP treatment in HCCs with ChIP data for TEAD occupancy in liver cancer cells (see Figure S4E and Experimental Procedures). To this end, we calculated enrichment for the YAP activation signature for each of the 111 HCC patients included in our human cohort. Correspondingly, nearest template prediction (NTP) revealed that the YAP gene-expression signature had a strong negative correlation with the *CTNNB1* mutation signature in this set of human HCCs (Lachenmayer et al., 2012; Figure 7A). We corroborated these findings using three additional, independent HCC classification systems (Figures S7A–S7C). Moreover, patients who were positive for the YAP expression signature showed strong enrichment in the "proliferation," poor-prognosis gene-expression subtype of HCC (Figures 7B and S7A; Chiang et al., 2008). In addition, YAP levels showed a close correlation with an E2F target gene/proliferation signature across both HCC cell lines and human specimens (Figures S7D and S7E) Together, these data suggest that YAP specifically contributes to the growth of an aggressive *CTNNB1* WT subtype of human HCC, and point to the potential therapeutic value of targeting Yap in these currently intractable tumors.

DISCUSSION

We have shown that siRNA-LNP-mediated inhibition of YAP is an effective therapeutic in a GEM model of advanced HCC. In response to YAP inactivation, tumor cells underwent rapid proliferative arrest and subsequently acquired features of hepatocyte differentiation. These findings demonstrate the potential of YAP as a drug target in HCC and suggest a paradigm for differentiation therapy in the treatment of this aggressive epithelial malignancy.

Whereas YAP activation can induce anti-apoptotic genes and enhance cell survival in multiple contexts, including livers treated with FAS ligand (Camargo et al., 2007; Zhou et al., 2009), we found no evidence of cell death upon siYAP-LNP administration in our HCC model. Rather, we observed inhibition of E2F target genes and a pronounced reduction in cell proliferation followed by a gradual activation of a hepatocyte differentiation program, culminating in the morphologic differentiation of the HCCs into nodules resembling regenerative hepatocytes. Thus, YAP inhibition in advanced HCC results in a remarkable reversion of transformed cells toward a growth-arrested and histopathologically benign phenotype.

Anti-cancer drug development efforts have focused largely on identifying agents that incite death of the tumor cells. An alternative approach is to attempt to instruct cancer cells to reactivate differentiation programs, thereby abrogating self-renewal and a replicative lifespan. This approach is presently being used successfully to treat acute promyelocytic leukemia harboring the *PML/RARA* fusion gene, where all-*trans* retinoic acid and arsenic trioxide induce terminal differentiation of the leukemic cells into mature granulocytes and block their self-renewal (de Thé and Chen, 2010). Whether adult epithelial malignancies retain a latent capacity to differentiate and whether distinct nodes in cell regulation can be identified as targets to restore this differentiation potential are key questions for the broader application of such strategies. Our work provides a proof-of-concept for this approach in an autochthonous model of aggressive HCC and identifies YAP as such a targetable node. Since differentiated hepatocytes survive for an extended period of time, it remains to be seen whether a durable response can be attained via YAP targeting or whether sustained inhibition or combination therapies are required. Notably, pharmacologic inhibition of YAP was recently shown to induce differentiation and tumor regression in embryonal rhabdomyosarcoma xenografts, suggesting that this approach may extend to multiple cancer types (Tremblay et al., 2014).

Our transcriptomic analyses linked YAP activity in the normal liver and HCC to the negative regulation of targets of HNF4A

(F) Quantification of KI67 staining at day 9. The chart shows the percentage of KI67+ HCC cells in different tumor nodules grouped according to the degree of YAP knockdown. Note that the decrease in KI67 staining correlates with effectiveness of YAP knockdown. siLuc-LNP: n = 20 tumors from 3 treated mice; siYAP-LNP: n = 34 tumors from 4 treated mice. Error bars indicate SEM. $^{**}p < 0.01$, $^{****}p < 0.0001$.

(G and H) GSEA of differentially expressed genes in response to siYAP-LNPs versus control siLuc-LNPs (day 9).

(G) Cell-cycle genes are repressed.

(H) Left: markers of hepatocyte differentiation are induced. Right: heatmap showing induction of markers specific to pericentral hepatocytes (Braeuning et al., 2006). NES, normalized enrichment score; FDR, false-discovery rate.

(I) By day 9, siYAP-LNPs result in loss of SOX9 staining, nuclear translocation of β-CATENIN, and induction of GS. Scale bar, 20 μm (H&E [right] and β-catenin) and 100 μm (H&E [left], YAP, SOX9, and GS).

See also Figure S4 and Table S2.

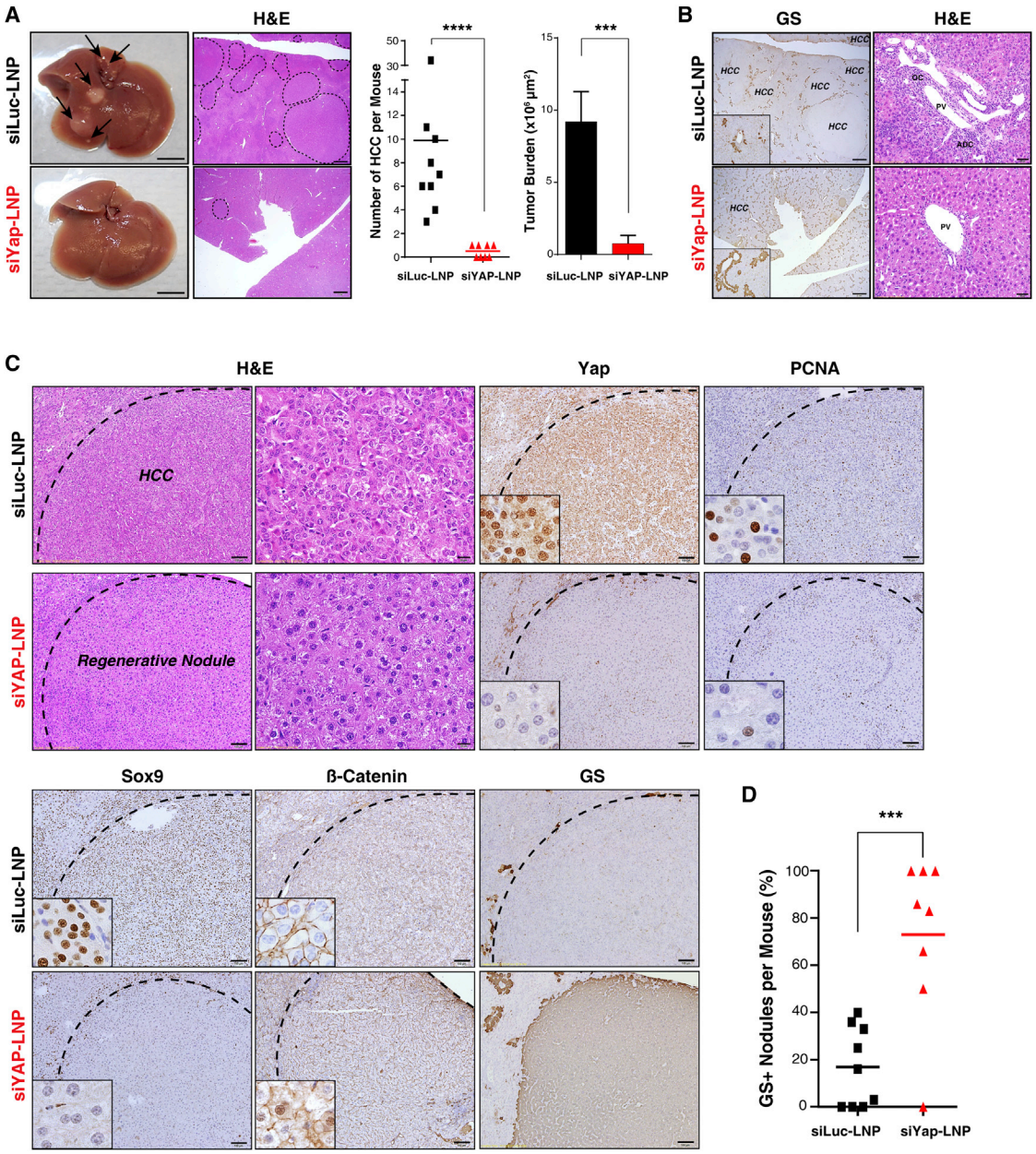

Figure 5. siLNP-Mediated YAP Silencing Is an Effective Differentiation Therapy for Advanced HCC

Following detection of tumors by US imaging, DKO^{Ad} mice were treated with siRNA-LNPs for 28 days and then euthanized.

(A) Representative gross liver images and H&E-stained sections. Arrows: visible liver tumors; dotted lines: histologically confirmed HCC lesions. The charts show the number of histologically validated HCC lesions/mouse (left) and tumor area occupied per whole liver cross-section (right; see Experimental Procedures). n = 9 mice (siLuc-LNP) and 8 mice (siYAP-LNP). Scale bars, 5 mm (gross) and 1 mm (H&E). Error bars indicate SEM. ***p < 0.001, ****p < 0.0001.

(B) The liver parenchyma shows a restoration of zonal GS expression and disappearance of ADCs upon siYAP-LNP treatment. HCC lesions are indicated. Scale bars, 1 µm (GS) and 50 µm (H&E).

(C) siYAP-LNP treatment results in replacement of invasive HCCs by benign nodules with histopathologic features consistent with differentiation to regenerative hepatocytes, associated with loss of SOX9, infrequent PCNA staining, focal induction of nuclear β-CATENIN, and strong upregulation of GS. Scale bars, 100 µm and 20 µm (H&E right panel).

(D) Chart quantifying the proportion of nodules that stained positive for GS. Error bars indicate SEM. ***p < 0.001.

See also Figure S5.

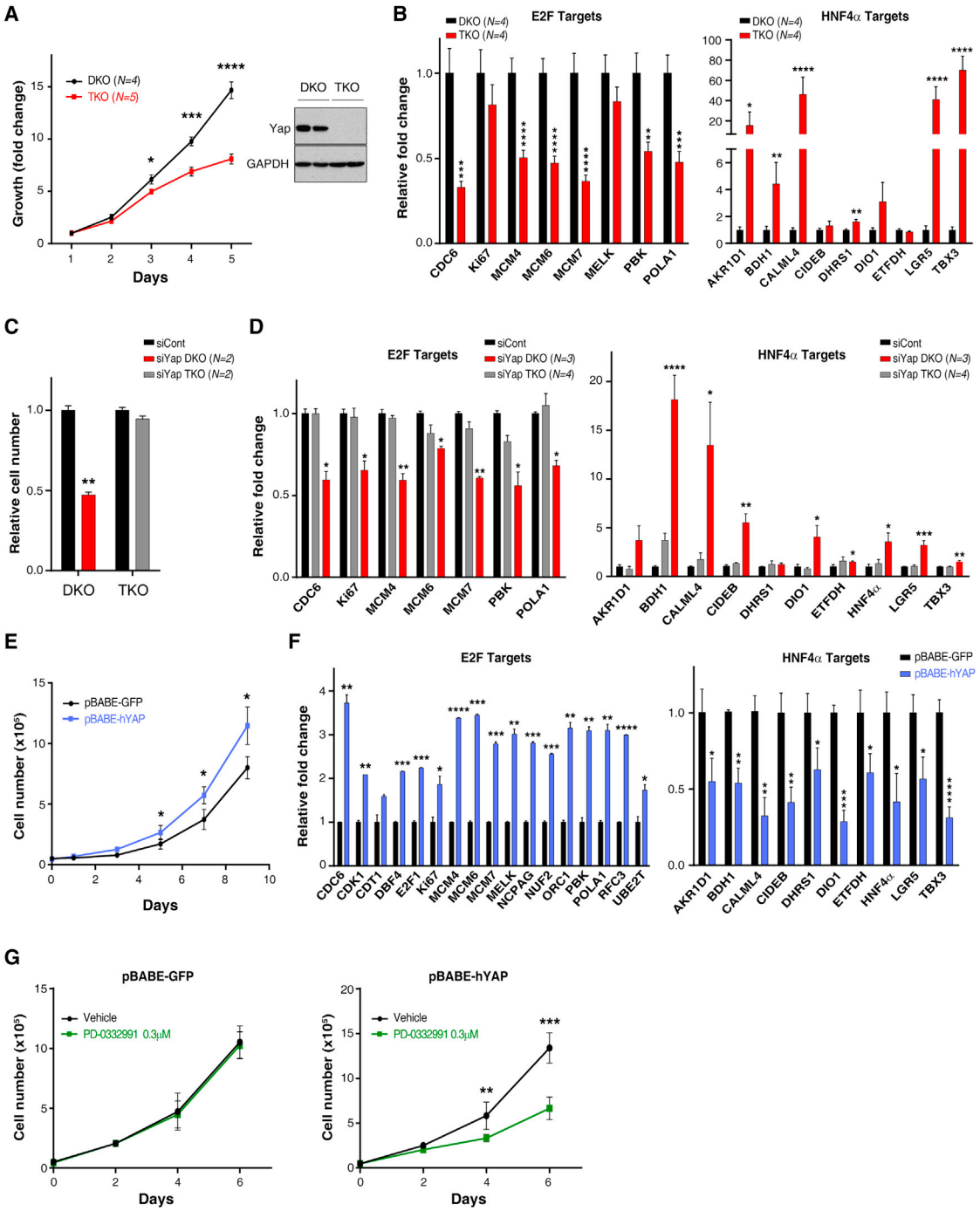

Figure 6. YAP Positively Regulates an E2F Proliferation Program and Suppresses the Hnf4α Hepatocyte Differentiation Pathway

(A) Left panel: early-passage HCC cultures derived from DKO mice display a proliferative advantage compared with TKO lines. N, number of independent cultures tested in each group. Right panel: western blot analysis confirming that YAP expression is restricted to the DKO lines.

(B) qRT-PCR analysis shows that DKO lines are characterized by higher basal expression of E2F targets (left panel) and lower expression of HNF4α targets (right panel). Error bars indicate SEM. *p < 0.05, **p < 0.01, ***p < 0.001, ****p < 0.0001.

(C and D) DKO and TKO cell lines were transfected with siRNA against YAP or control siRNA.

(C) Quantification of cell growth data showing that siRNA-mediated YAP knockdown causes proliferative arrest of DKO lines but does not affect TKO cells.

(D) qRT-PCR analysis showing that YAP knockdown in DKO cells results in a significant decrease in the expression of multiple E2F-regulated cell-cycle genes (left panel) and pronounced activation of HNF4A targets (right panel). Error bars indicate SEM. *p < 0.05, **p < 0.01, ***p < 0.001, ****p < 0.0001.

(E–G) TKO cells were transduced with retroviruses expressing human YAP (hYAP) or GFP control.

(legend continued on next page)

and FOXA2/FOXA1. It is notable that the differentially expressed genes harboring TEAD binding sites—and thus potential direct YAP targets—exhibited a striking enrichment for HNF4A and FOXA1 binding sites (Figure S4E). Although further studies will be required to resolve the associated transcriptional circuitry, these results suggest that the reported functions of YAP in switching the occupancy of HNF4A/FOXA1 from enhancers of mature hepatocyte genes to those of hepatic progenitor genes (Schaub et al., 2014) may also be operative in dictating sustained tumorigenic growth versus hepatocyte differentiation in advanced HCC. Accordingly, deletion of *Hnf4a* in the adult mouse liver leads to phenotypes overlapping those observed upon YAP activation, including loss of hepatocyte identity, proliferation of dedifferentiated hepatocytes, and expansion of ADCs (Bonzo et al., 2012; Saha et al., 2014; Walesky et al., 2013). We also found that expression of E2F target genes is positively associated with YAP function in vivo (Figures S4D, S7D, and S7E), consistent with prior work demonstrating cooperative interactions between YAP and E2F in the liver (Ehmer et al., 2014). Notably, we observed YAP-mediated modulation of HNF4A targets and E2F targets in vitro using primary HCC cultures, suggesting that the regulatory interactions may be direct (Figure 6). YAP activity was also associated with SOX9 expression and inhibition of β-CATENIN nuclear translocation, although these pathways were not as prominently altered in vitro (data not shown).

Our studies provide a number of insights into the role of Hippo/YAP in controlling cell fate in the adult liver. In the normal liver, we found that nuclear YAP was expressed at the highest levels in the bile ducts and showed a decreasing gradient of expression along the porto-central axis, with the final row of pericentral hepatocytes completely lacking YAP expression (Figures 1A and 1B). Activation of endogenous YAP following acute *Mst1*/*Mst2* deletion not only resulted in conversion of hepatocytes in the periportal area to ADCs but also overrode the zonation program in pericentral hepatocytes, as reflected by the loss of expression of GS and OAT (Figures 2A and 2C; also see Figures 1C, 1D, and S1D for the *Alb-Cre* model). Moreover, acute deletion of YAP caused aberrant expansion of the GS+ domain to multiple layers of pericentral hepatocytes (Figures 2A and 2C). Therefore, we have demonstrated an unexpected role for basal YAP function in maintaining liver zonation, and showed that the differentiation state of pericentral hepatocytes is sensitive to precise tuning of YAP activity (Figure 7C). Liver zonation is an intriguing mechanism for regional compartmentalization of metabolic functions (Jungermann and Katz, 1989; Torre et al., 2011), and our data establish YAP as a major determinant of zonal identity with a role opposing that of β-CATENIN, which activates a pericentral program. It will be of interest to determine the basis for graded YAP activity within the parenchyma and to specifically relate YAP function to the control of the diverse metabolic processes carried out by this organ.

Although Yap deletion delayed tumorigenesis in DKO mice, it did not completely prevent the formation of HCC. Rather, all of the DKO Yap+/− and TKO animals eventually developed invasive HCC. These data are consistent with MST1/MST2 acting to suppress HCC development through targets in addition to YAP. It is possible that TAZ, which is expressed in the HCCs and derivative cell lines (data not shown), partially compensates for YAP inactivation in this context. Since YAP deficiency eliminated ADCs in TKO mice and resulted in a distinct tumor phenotype (well-differentiated histology, β-CATENIN+, GS+, and SOX9−; Figures 3D and 7C), it appears that this secondary pathway does not fully recapitulate the broad reprogramming of hepatocyte differentiation induced by YAP.

The link between YAP activity and differentiation status in HCC appears to be relevant in the corresponding human tumors as well. Using the transcriptional alterations provoked by YAP inactivation in our HCC model as a readout for YAP activity, we found that the YAP signature was negatively correlated with the *CTNNB1* mutant subclass of HCC and positively correlated with the "proliferation" subclass (Figures 7A, 7B, and S7A–S7C). These data extend findings from IHC analysis that showed an inverse correlation between nuclear YAP and nuclear β-CATENIN (Tao et al., 2014), and point to a molecular subtype of HCC that may benefit from anti-YAP therapies.

The idea of targeting YAP as a cancer therapy is particularly compelling due to the clear dosage dependence of its oncogenic activity. Approaches to inhibit YAP using small molecules and peptides have been described (Jiao et al., 2014; Liu-Chittenden et al., 2012). Our data suggest that there may be a clinical path forward using siYAP-LNPs to treat primary HCC. Importantly, as a genetically targeted therapy, siYAP-LNPs would be expected to have more specificity and lower toxicity than most small-molecule inhibitors, and indeed, we observed mild and reversible side effects in our studies (Figures S5B–S5D). Finally, siRNA-LNPs can readily be adapted to inhibit multiple targets, enabling the development of combinatorial strategies.

EXPERIMENTAL PROCEDURES

Mouse Models

Mice were housed in pathogen-free animal facilities at Massachusetts General Hospital (MGH). All experiments were conducted under protocol 2005N000148, approved by the Subcommittee on Research Animal Care at MGH. The following mouse strains were used: *Mst1*$^{-}$, *Mst2*^{Flox}, *Yap*^{Flox}, and *Albumin-Cre* (Postic and Magnuson, 2000; Schlegelmilch et al., 2011; Zhou et al., 2009). The *Albumin-Cre* transgene efficiently deletes floxed sequences in all liver lineages by 4–6 weeks of age. Mice were maintained on a mixed genetic background and each genotype was generated from intercrosses from the same colony. For Adeno-Cre studies, 5×10^9 pfu of CMV-Cre adenovirus resuspended in a final volume of 200 μl PBS was injected into the tail vein of 6-week-old mice. All mice included in the survival analysis were euthanized when criteria for disease burden were reached (including abdominal

(E) YAP expression significantly increases the proliferation of TKO cells (left panel).
(F) Forced expression of YAP induces E2F targets (left panel) and inhibits HNF4A targets (right panel). Error bars indicate SEM. *p < 0.05, **p < 0.01, ***p < 0.001, ****p < 0.0001.
(G) Treatment with a CDK4/6 inhibitor (PD-0332991, 0.3 μM) impairs the proliferation of TKO cells expressing YAP (right panel) without affecting GFP-expressing TKO control cells (left panel). Error bars indicate SEM. **p < 0.01, ***p < 0.001.
See also Figure S6.

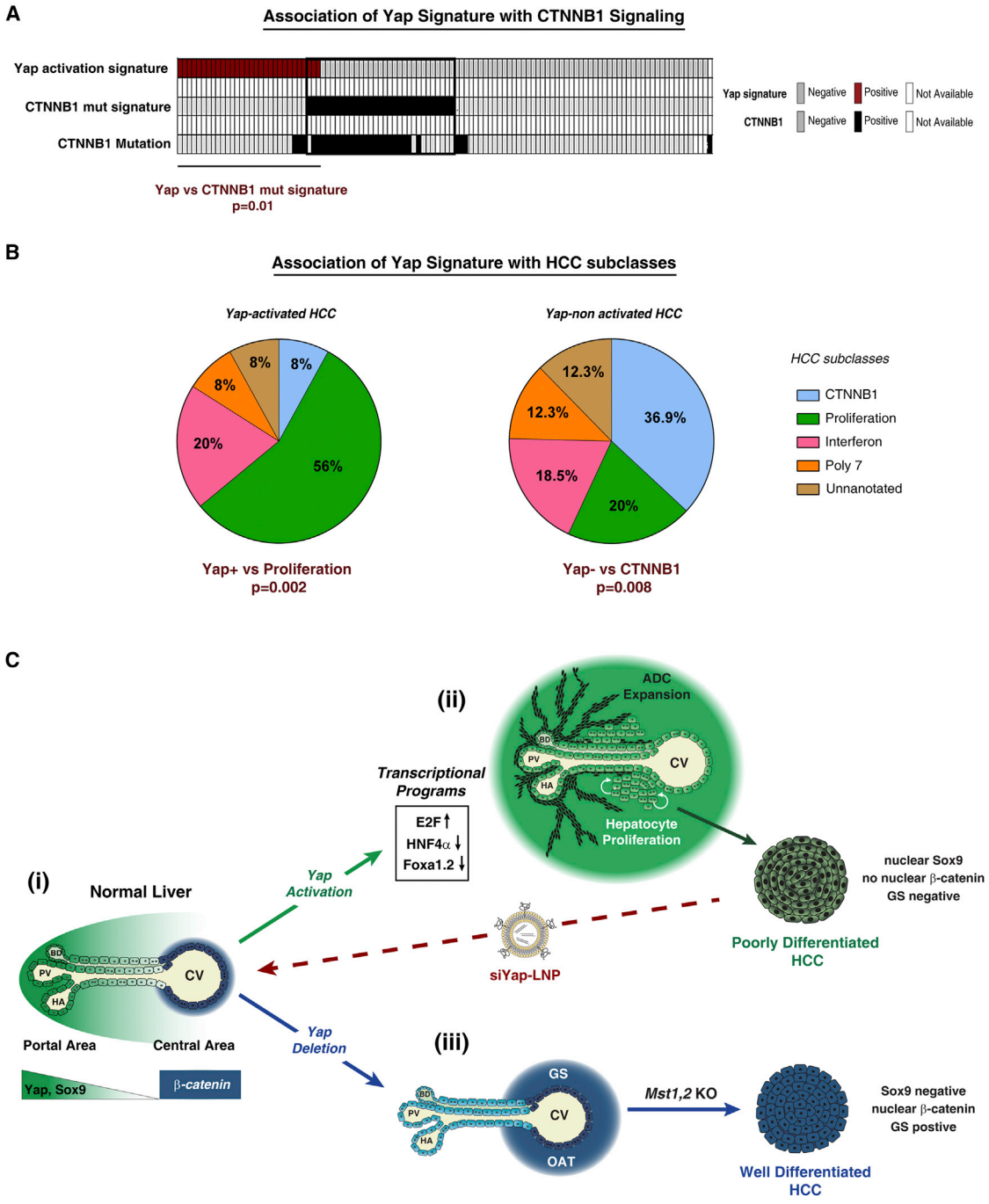

Figure 7. The YAP Activity Signature Is Enriched in Human HCC Subtypes Defined by a Lack of the CTNNB1 Mutation and a Proliferation Gene Profile

(A) Analysis of 111 human HCC specimens reveals an inverse correlation between the *CTNNB1* mutation signature and a YAP activation signature.

(B) Using a second HCC classification system (Chiang et al., 2008), the YAP activation signature (YAP+) is positively correlated with the aggressive "proliferation" subclass, whereas absence of the signature (YAP−) significantly correlates with the *CTNNB1* subclass. Fisher's exact test was used for statistical analysis.

(C) Model illustrating the impact of Hippo/YAP modulation on liver biology. (i) In normal liver, YAP shows a decreasing gradient of nuclear and cytoplasmic expression along the porto-central axis. The final layer of hepatocytes adjacent to the central vein completely lacks YAP expression, whereas active β-catenin and GS are restricted to these cells. (ii) Activation of YAP in hepatocytes results in induction of proliferation-related E2F target genes, down-regulation of the targets of the HNF4A and FOXA1,2, and loss of pericentral β-CATENIN targets (e.g., GS and OAT), as well as hepatocyte proliferation throughout the lobule and dedifferentiation of hepatocytes to ADCs in the portal area. The resulting HCCs are poorly differentiated, express SOX9, and lack nuclear β-CATENIN and its target, GS. Treatment with siYAP-LNPs leads to tumor regression and hepatocyte differentiation. (iii) Yap deletion leads to an

(legend continued on next page)

distension that impeded movement, loss of >15% of body weight, labored breathing, and/or abnormal posture).

Human Tumor Specimens

Resected human tumor tissue was collected from the Biorepository Tissue Bank at the Icahn School of Medicine at Mount Sinai (New York) after approval by the institutional review board (IRB) committee.

siLNP Formulations

LNPs were formed by mixing equal volumes of lipids dissolved in alcohol (lipid solution containing a cationic lipid, a helper lipid [cholesterol], a neutral lipid [DSPC], and a PEG lipid), with siRNA (dissolved in sodium citrate [sodium chloride buffer], pH 4.0) by an impinging jet process. Following an incubation period, the solution was concentrated and diafiltered by an ultrafiltration process using membranes with a molecular weight cutoff of 100 kDa. The product was sterile filtered and stored at 4°C. The total siRNA was determined by anion exchange chromatography. The targeted sequences for Yap were 5′-TTAAGAAGTATCTTTGACC-3′ (siYap-LNP #1) and 5′-TTAAGAAAGGGA TCGGAAC-3′ (siYap-LNP #2). A formulation targeting luciferase (siLuc-LNP) was used as a control. Formulations were intravenously injected (via tail vein) at 3 mg/kg per injection every other day (for short-term treatment, i.e., <10 days of treatment) or for 3 consecutive days with a resting period of 2 days between every round of treatment for long-term analysis.

GSEA

We used GSEA (http://www.broadinstitute.org/gsea/index.jsp) of the expression data to assess enrichment of gene signatures. Depending on the data set, we used several different methods to rank genes. In the siRNA-LNP studies, we performed a pairwise GSEA by creating ranked lists of genes using the log2 ratio of siYAP-LNPs to siLuc-LNPs, and obtained p values by permuting the gene set. To identify direct target genes (Figures S2B and S4E), we downloaded TEAD ChIP peaks for HEPG2 cells from ENCODE (http://genome.ucsc.edu/ENCODE/) and generated TEAD-target lists by associating genes with TEAD peaks using PeakAnalyzer (Salmon-Divon et al., 2010) with the "closest-TSS" routine. We defined YAP signatures by comparing the differentially regulated genes in D8 or D9 and TEAD targets. For transcription factor enrichment analysis, we utilized the ENCODE ChIP-seq significance tool (Auerbach et al., 2013). In brief, YAP-TEAD lists for D8 or D9 were uploaded in the web interface (http://encodeqt.simple-encode.org) and transcription factor binding sites were detected in the region +5,000 bp to −2,500 bp relative to the TSS of each gene. We calculated the significance of enrichment of a transcription factor using the hypergeometric test and corrected for multiple testing using the Benjamini-Hochberg false-discovery rate (FDR).

ACCESSION NUMBERS

The NCBI GEO accession number for the data reported in this paper is GSE65665.

SUPPLEMENTAL INFORMATION

Supplemental Information includes Supplemental Experimental Procedures, seven figures, and three tables and can be found with this article online at http://dx.doi.org/10.1016/j.celrep.2015.02.027.

AUTHOR CONTRIBUTIONS

J.F., S.B., L.R., and N.B. designed experiments. J.F. performed experiments with the assistance of F.K., S.B., H.S.T., N.C., C.A.P., J.M.N., R.M.P., M.L., B.M., and G.C. J.F., F.K., S.B., V.D., A.X.Z., A.L., Y.H., J.A., D.S., A.I.M., J.M.L., D.M., L.R., and N.B. analyzed the data. F.K. and S.B. contributed equally. J.F. and N.B. wrote the manuscript.

ACKNOWLEDGMENTS

We thank members of the Bardeesy lab, A. Kimmelman, and W. Kim for helpful comments, and F. Camargo for generously providing the Yap^{fl} mice. We also thank the Novartis siRNA formulation group for preparing the siLNPs, K. Ross for bioinformatics assistance, and D. Zhou for initiation of the mouse cohort. This work was supported by grants from the NIH/NCI (R01CA136567 and P50CA127003 to N.B. and J.A.), NIH/NIDDK (R01DK099558 to Y.H.), and the TargetCancer Foundation (to N.B.). N.B. holds the Gallagher Chair in Gastrointestinal Cancer Research at Massachusetts General Hospital. N.B. and J.M.L. are members of the Waxman Institute without Walls. J.F. and S.B. are recipients of long-term postdoctoral fellowships from EMBO and the International Human Frontiers Science Program, respectively, and both were supported by ECOR Fund for Medical Discovery postdoctoral fellowships. C.P. is the recipient of a CIHR postdoctoral fellowship. J.M.L. and D.S. are supported by the Asociación Española Contra el Cáncer. A.L., B.M., D.M., and L.R. are employees of Novartis, and J.M.L. is a consultant with Novartis. This work is dedicated to the bright memory of Rolande Fitamant (1959–2014).

Received: December 1, 2014
Revised: January 16, 2015
Accepted: February 6, 2015
Published: March 10, 2015

REFERENCES

Alder, O., Cullum, R., Lee, S., Kan, A.C., Wei, W., Yi, Y., Garside, V.C., Bilenky, M., Griffith, M., Morrissy, A.S., et al. (2014). Hippo signaling influences HNF4A and FOXA2 enhancer switching during hepatocyte differentiation. Cell Rep. *9*, 261–271.

Antoniou, A., Raynaud, P., Cordi, S., Zong, Y., Tronche, F., Stanger, B.Z., Jacquemin, P., Pierreux, C.E., Clotman, F., and Lemaigre, F.P. (2009). Intrahepatic bile ducts develop according to a new mode of tubulogenesis regulated by the transcription factor SOX9. Gastroenterology *136*, 2325–2333.

Auerbach, R.K., Chen, B., and Butte, A.J. (2013). Relating genes to function: identifying enriched transcription factors using the ENCODE ChIP-Seq significance tool. Bioinformatics *29*, 1922–1924.

Benhamouche, S., Decaens, T., Godard, C., Chambrey, R., Rickman, D.S., Moinard, C., Vasseur-Cognet, M., Kuo, C.J., Kahn, A., Perret, C., and Colnot, S. (2006). Apc tumor suppressor gene is the "zonation-keeper" of mouse liver. Dev. Cell *10*, 759–770.

Benhamouche, S., Curto, M., Saotome, I., Gladden, A.B., Liu, C.H., Giovannini, M., and McClatchey, A.I. (2010). Nf2/Merlin controls progenitor homeostasis and tumorigenesis in the liver. Genes Dev. *24*, 1718–1730.

Bochkis, I.M., Schug, J., Ye, D.Z., Kurinna, S., Stratton, S.A., Barton, M.C., and Kaestner, K.H. (2012). Genome-wide location analysis reveals distinct transcriptional circuitry by paralogous regulators Foxa1 and Foxa2. PLoS Genet. *8*, e1002770.

Bonzo, J.A., Ferry, C.H., Matsubara, T., Kim, J.H., and Gonzalez, F.J. (2012). Suppression of hepatocyte proliferation by hepatocyte nuclear factor 4α in adult mice. J. Biol. Chem. *287*, 7345–7356.

Braeuning, A., Ittrich, C., Köhle, C., Hailfinger, S., Bonin, M., Buchmann, A., and Schwarz, M. (2006). Differential gene expression in periportal and perivenous mouse hepatocytes. FEBS J. *273*, 5051–5061.

expansion of β-CATENIN targets in the central area. Additionally, Yap ablation completely blocks hepatocyte proliferation and oval cell expansion resulting from *Mst1*/*Mst2* loss, and delays HCC development. The HCCs that develop display distinct differentiation markers and histopathology as compared with Yap-driven HCCs.

ADC, atypical ductal cell; BD, bile duct; CV, central vein; GS, glutamine synthetase; HA, hepatic artery; OAT, ornithine aminotransferase; PV, portal vein. See also Figure S7.

Camargo, F.D., Gokhale, S., Johnnidis, J.B., Fu, D., Bell, G.W., Jaenisch, R., and Brummelkamp, T.R. (2007). YAP1 increases organ size and expands undifferentiated progenitor cells. Curr. Biol. *17*, 2054–2060.

Cheng, A.L., Kang, Y.K., Chen, Z., Tsao, C.J., Qin, S., Kim, J.S., Luo, R., Feng, J., Ye, S., Yang, T.S., et al. (2009). Efficacy and safety of sorafenib in patients in the Asia-Pacific region with advanced hepatocellular carcinoma: a phase III randomised, double-blind, placebo-controlled trial. Lancet Oncol. *10*, 25–34.

Chiang, D.Y., Villanueva, A., Hoshida, Y., Peix, J., Newell, P., Minguez, B., LeBlanc, A.C., Donovan, D.J., Thung, S.N., Solé, M., et al. (2008). Focal gains of VEGFA and molecular classification of hepatocellular carcinoma. Cancer Res. *68*, 6779–6788.

de Thé, H., and Chen, Z. (2010). Acute promyelocytic leukaemia: novel insights into the mechanisms of cure. Nat. Rev. Cancer *10*, 775–783.

Dong, J., Feldmann, G., Huang, J., Wu, S., Zhang, N., Comerford, S.A., Gayyed, M.F., Anders, R.A., Maitra, A., and Pan, D. (2007). Elucidation of a universal size-control mechanism in Drosophila and mammals. Cell *130*, 1120–1133.

Ehmer, U., Zmoos, A.F., Auerbach, R.K., Vaka, D., Butte, A.J., Kay, M.A., and Sage, J. (2014). Organ size control is dominant over Rb family inactivation to restrict proliferation in vivo. Cell Rep. *8*, 371–381.

El-Serag, H.B. (2011). Hepatocellular carcinoma. N. Engl. J. Med. *365*, 1118–1127.

Forner, A., Llovet, J.M., and Bruix, J. (2012). Hepatocellular carcinoma. Lancet *379*, 1245–1255.

Fujimoto, A., Totoki, Y., Abe, T., Boroevich, K.A., Hosoda, F., Nguyen, H.H., Aoki, M., Hosono, N., Kubo, M., Miya, F., et al. (2012). Whole-genome sequencing of liver cancers identifies etiological influences on mutation patterns and recurrent mutations in chromatin regulators. Nat. Genet. *44*, 760–764.

Ganem, N.J., Cornils, H., Chiu, S.Y., O'Rourke, K.P., Arnaud, J., Yimlamai, D., Théry, M., Camargo, F.D., and Pellman, D. (2014). Cytokinesis failure triggers hippo tumor suppressor pathway activation. Cell *158*, 833–848.

Gougelet, A., Torre, C., Veber, P., Sartor, C., Bachelot, L., Denechaud, P.D., Godard, C., Moldes, M., Burnol, A.F., Dubuquoy, C., et al. (2014). T-cell factor 4 and β-catenin chromatin occupancies pattern zonal liver metabolism in mice. Hepatology *59*, 2344–2357.

Guichard, C., Amaddeo, G., Imbeaud, S., Ladeiro, Y., Pelletier, L., Maad, I.B., Calderaro, J., Bioulac-Sage, P., Letexier, M., Degos, F., et al. (2012). Integrated analysis of somatic mutations and focal copy-number changes identifies key genes and pathways in hepatocellular carcinoma. Nat. Genet. *44*, 694–698.

Harvey, K.F., Zhang, X., and Thomas, D.M. (2013). The Hippo pathway and human cancer. Nat. Rev. Cancer *13*, 246–257.

Hoshida, Y., Nijman, S.M., Kobayashi, M., Chan, J.A., Brunet, J.P., Chiang, D.Y., Villanueva, A., Newell, P., Ikeda, K., Hashimoto, M., et al. (2009). Integrative transcriptome analysis reveals common molecular subclasses of human hepatocellular carcinoma. Cancer Res. *69*, 7385–7392.

Jiao, S., Wang, H., Shi, Z., Dong, A., Zhang, W., Song, X., He, F., Wang, Y., Zhang, Z., Wang, W., et al. (2014). A peptide mimicking VGLL4 function acts as a YAP antagonist therapy against gastric cancer. Cancer Cell *25*, 166–180.

Jungermann, K., and Katz, N. (1989). Functional specialization of different hepatocyte populations. Physiol. Rev. *69*, 708–764.

Lachenmayer, A., Alsinet, C., Savic, R., Cabellos, L., Toffanin, S., Hoshida, Y., Villanueva, A., Minguez, B., Newell, P., Tsai, H.W., et al. (2012). Wnt-pathway activation in two molecular classes of hepatocellular carcinoma and experimental modulation by sorafenib. Clin. Cancer Res. *18*, 4997–5007.

Lee, K.P., Lee, J.H., Kim, T.S., Kim, T.H., Park, H.D., Byun, J.S., Kim, M.C., Jeong, W.I., Calvisi, D.F., Kim, J.M., and Lim, D.S. (2010). The Hippo-Salvador pathway restrains hepatic oval cell proliferation, liver size, and liver tumorigenesis. Proc. Natl. Acad. Sci. USA *107*, 8248–8253.

Li, Z., Tuteja, G., Schug, J., and Kaestner, K.H. (2012). Foxa1 and Foxa2 are essential for sexual dimorphism in liver cancer. Cell *148*, 72–83.

Liu-Chittenden, Y., Huang, B., Shim, J.S., Chen, Q., Lee, S.J., Anders, R.A., Liu, J.O., and Pan, D. (2012). Genetic and pharmacological disruption of the TEAD-YAP complex suppresses the oncogenic activity of YAP. Genes Dev. *26*, 1300–1305.

Llovet, J.M., Ricci, S., Mazzaferro, V., Hilgard, P., Gane, E., Blanc, J.F., de Oliveira, A.C., Santoro, A., Raoul, J.L., Forner, A., et al.; SHARP Investigators Study Group. (2008). Sorafenib in advanced hepatocellular carcinoma. N. Engl. J. Med. *359*, 378–390.

Lu, L., Li, Y., Kim, S.M., Bossuyt, W., Liu, P., Qiu, Q., Wang, Y., Halder, G., Finegold, M.J., Lee, J.S., and Johnson, R.L. (2010). Hippo signaling is a potent in vivo growth and tumor suppressor pathway in the mammalian liver. Proc. Natl. Acad. Sci. USA *107*, 1437–1442.

Mo, J.S., Park, H.W., and Guan, K.L. (2014). The Hippo signaling pathway in stem cell biology and cancer. EMBO Rep. *15*, 642–656.

Postic, C., and Magnuson, M.A. (2000). DNA excision in liver by an albumin-Cre transgene occurs progressively with age. Genesis *26*, 149–150.

Saha, S.K., Parachoniak, C.A., Ghanta, K.S., Fitamant, J., Ross, K.N., Najem, M.S., Gurumurthy, S., Akbay, E.A., Sia, D., Cornella, H., et al. (2014). Mutant IDH inhibits HNF-4α to block hepatocyte differentiation and promote biliary cancer. Nature *513*, 110–114.

Salmon-Divon, M., Dvinge, H., Tammoja, K., and Bertone, P. (2010). PeakAnalyzer: genome-wide annotation of chromatin binding and modification loci. BMC Bioinformatics *11*, 415.

Schaub, J.R., Malato, Y., Gormond, C., and Willenbring, H. (2014). Evidence against a stem cell origin of new hepatocytes in a common mouse model of chronic liver injury. Cell Rep. *8*, 933–939.

Schlegelmilch, K., Mohseni, M., Kirak, O., Pruszak, J., Rodriguez, J.R., Zhou, D., Kreger, B.T., Vasioukhin, V., Avruch, J., Brummelkamp, T.R., and Camargo, F.D. (2011). Yap1 acts downstream of α-catenin to control epidermal proliferation. Cell *144*, 782–795.

Shin, S., Walton, G., Aoki, R., Brondell, K., Schug, J., Fox, A., Smirnova, O., Dorrell, C., Erker, L., Chu, A.S., et al. (2011). Foxl1-Cre-marked adult hepatic progenitors have clonogenic and bilineage differentiation potential. Genes Dev. *25*, 1185–1192.

Tao, J., Calvisi, D.F., Ranganathan, S., Cigliano, A., Zhou, L., Singh, S., Jiang, L., Fan, B., Terracciano, L., Armeanu-Ebinger, S., et al. (2014). Activation of β-catenin and Yap1 in human hepatoblastoma and induction of hepatocarcinogenesis in mice. Gastroenterology *147*, 690–701.

Torre, C., Perret, C., and Colnot, S. (2011). Transcription dynamics in a physiological process: β-catenin signaling directs liver metabolic zonation. Int. J. Biochem. Cell Biol. *43*, 271–278.

Tremblay, A.M., Missiaglia, E., Galli, G.G., Hettmer, S., Urcia, R., Carrara, M., Judson, R.N., Thway, K., Nadal, G., Selfe, J.L., et al. (2014). The Hippo transducer YAP1 transforms activated satellite cells and is a potent effector of embryonal rhabdomyosarcoma formation. Cancer Cell *26*, 273–287.

Tschaharganeh, D.F., Chen, X., Latzko, P., Malz, M., Gaida, M.M., Felix, K., Ladu, S., Singer, S., Pinna, F., Gretz, N., et al. (2013). Yes-associated protein up-regulates Jagged-1 and activates the Notch pathway in human hepatocellular carcinoma. Gastroenterology *144*, 1530–1542.

Walesky, C., Gunewardena, S., Terwilliger, E.F., Edwards, G., Borude, P., and Apte, U. (2013). Hepatocyte-specific deletion of hepatocyte nuclear factor-4α in adult mice results in increased hepatocyte proliferation. Am. J. Physiol. Gastrointest. Liver Physiol. *304*, G26–G37.

Whitehead, K.A., Langer, R., and Anderson, D.G. (2009). Knocking down barriers: advances in siRNA delivery. Nat. Rev. Drug Discov. *8*, 129–138.

Xu, M.Z., Yao, T.J., Lee, N.P., Ng, I.O., Chan, Y.T., Zender, L., Lowe, S.W., Poon, R.T., and Luk, J.M. (2009). Yes-associated protein is an independent prognostic marker in hepatocellular carcinoma. Cancer *115*, 4576–4585.

Yanger, K., Zong, Y., Maggs, L.R., Shapira, S.N., Maddipati, R., Aiello, N.M., Thung, S.N., Wells, R.G., Greenbaum, L.E., and Stanger, B.Z. (2013). Robust cellular reprogramming occurs spontaneously during liver regeneration. Genes Dev. *27*, 719–724.

Yanger, K., Knigin, D., Zong, Y., Maggs, L., Gu, G., Akiyama, H., Pikarsky, E., and Stanger, B.Z. (2014). Adult hepatocytes are generated by self-duplication rather than stem cell differentiation. Cell Stem Cell *15*, 340–349.

Yimlamai, D., Christodoulou, C., Galli, G.G., Yanger, K., Pepe-Mooney, B., Gurung, B., Shrestha, K., Cahan, P., Stanger, B.Z., and Camargo, F.D. (2014). Hippo pathway activity influences liver cell fate. Cell *157*, 1324–1338.

Yin, F., Yu, J., Zheng, Y., Chen, Q., Zhang, N., and Pan, D. (2013). Spatial organization of Hippo signaling at the plasma membrane mediated by the tumor suppressor Merlin/NF2. Cell *154*, 1342–1355.

Yu, F.X., and Guan, K.L. (2013). The Hippo pathway: regulators and regulations. Genes Dev. *27*, 355–371.

Zender, L., Spector, M.S., Xue, W., Flemming, P., Cordon-Cardo, C., Silke, J., Fan, S.T., Luk, J.M., Wigler, M., Hannon, G.J., et al. (2006). Identification and validation of oncogenes in liver cancer using an integrative oncogenomic approach. Cell *125*, 1253–1267.

Zhang, N., Bai, H., David, K.K., Dong, J., Zheng, Y., Cai, J., Giovannini, M., Liu, P., Anders, R.A., and Pan, D. (2010). The Merlin/NF2 tumor suppressor functions through the YAP oncoprotein to regulate tissue homeostasis in mammals. Dev. Cell *19*, 27–38.

Zhou, D., Conrad, C., Xia, F., Park, J.S., Payer, B., Yin, Y., Lauwers, G.Y., Thasler, W., Lee, J.T., Avruch, J., and Bardeesy, N. (2009). Mst1 and Mst2 maintain hepatocyte quiescence and suppress hepatocellular carcinoma development through inactivation of the Yap1 oncogene. Cancer Cell *16*, 425–438.